HHS Public Access

Author manuscript

*Photochem Photobiol*. Author manuscript; available in PMC 2020 January 01.

Published in final edited form as:

*Photochem Photobiol*. 2019 January ; 95(1): 119–125. doi:10.1111/php.12952.

# Apoptosis, Paraptosis and Autophagy: Death and Survival Pathways Associated with Photodynamic Therapy†

**David Kessel***

Wayne State University School of Medicine, Detroit MI 40201 USA

## Abstract

The ability of photosensitizing agents to create photodamage at specific sub-cellular sites has proved useful for characterizing pathway(s) to cell death and for selecting optimal targets for anti-tumor efficacy. Both apoptosis and autophagy can occur after photodamage directed at mitochondria, lysosomes or the ER, with the balance often a determinant of overall efficacy. A combination of lysosomal + mitochondrial targets is associated with enhanced efficacy. More recently, ER photodamage was found to evoke a mainly unexplored mode of photokilling that involves extensive cytoplasmic vacuole formation but does not represent autophagy. This has been termed ‘paraptosis’ and appears to be a reaction to the appearance of misfolded ER proteins. This report is designed to summarize current knowledge relating to death pathways and update information relating to paraptosis as a PDT response.

## Graphical abstract

Image of paraptosis showing the extensive series of cytoplasmic vacuoles 16 hr after irradiation of OVCAR-5 cells photosensitized with hypericin.

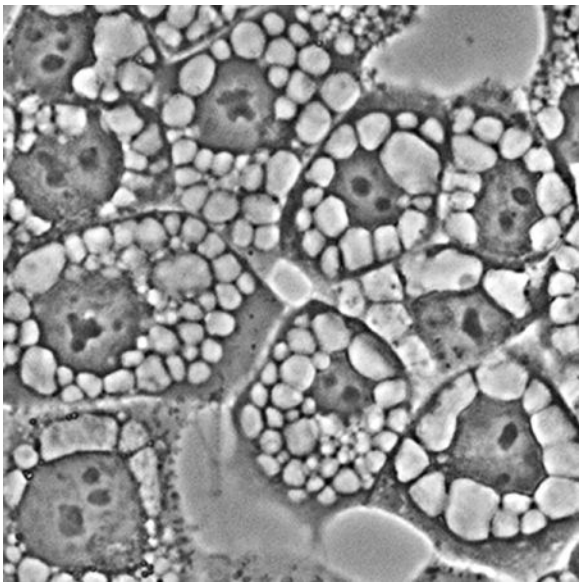

†This article is part of a Special Issue celebrating Photochemistry and Photobiology’s 55th Anniversary.

*Corresponding author’s: dhkessel@med.wayne.edu (David Kessel).

## INTRODUCTION

Photodynamic therapy (PDT) is both a selective means for tumor eradication and a technique for probing pathways leading to cell death. This effect is catalyzed by derivatives of porphyrins and related structures that are capable of preferentially sensitizing malignant cell types to light. The first reports involved a poorly-defined material termed HPD (hematoporphyrin derivative) [1]. The structure of this material was ultimately found to consist of a collection of monomeric and oligomeric porphyrin ethers and esters [2]. A purified form of HPD lacking the monomers is currently marketed under the name 'Photofrin'. Many photosensitizing agents have now been identified, often with superior properties. The phototoxic effect of PDT was traced to formation of reactive oxygen species (ROS) upon irradiation of photosensitized cells, principally $^1O_2$ and $^\bullet OH$ [3,4]. While high-dose PDT can evoke necrosis, this is usually to be avoided since selectivity may be lost. The degree of selectivity observed *in* vivo will depend, in part, on the ratio of photosensitizer accumulation in malignant vs. non-malignant tissues. Since this is unlikely to be several orders of magnitude, use of supra-lethal light doses is generally to be avoided. The mode of cellular photodamage that occurs after therapy often involves a death pathway termed apoptosis, a series of events that lead to nuclear and cellular fragmentation [5,6]. Another response to photodamage is autophagy, a process otherwise involved in the recycling of cellular components. Autophagy is more typically a response to starvation conditions, but in the context of PDT can be cytoprotective [7] or a factor in cell death [8]. There are now indications that tumor eradication can be enhanced when PDT is incorporated into 'combination' protocols. When chemotherapy or combinations of photosensitizers are involved, there is the possibility of retaining efficacy at reduced drug levels [9–12]. PDT can sensitize malignant cell types to both chemotherapy [12] and ionizing radiation [13].

While many chemical structures can utilize incident light for photodynamic processes, those useful for therapeutic purposes localize in neoplastic tissues and their vasculature for reasons still not entirely understood. Photofrin, the first of the photosensitizing agents to achieve widespread clinical use, also had the adverse effect of photosensitizing skin to incident light [14], a problem not usually encountered with 'second-generation' photosensitizing agents.

The ability of photosensitizing agents to target specific subcellular loci has been helpful in exploring death pathways in mammalian cell types. There are agents that can initiate photodamage to mitochondria, lysosomes, the ER, Golgi, plasma membranes and combinations of these sites. Characterization of new photosensitizing agents often involves assessing sites of sub-cellular localization. Based on recent studies involving structure-activity relations, we have proposed that an especially effective targeting combination involves both lysosomes and mitochondria [11]. These sub-cellular targets are within the targeting range of Photofrin [15], perhaps explaining the efficacy of a preparation with a relatively weak absorbance band at a wavelength (630 nm) relatively ineffective at penetrating tissue [16]. An agent with the targeting spectrum of Photofrin, but with a much greater absorbance band farther into the near-IR range could therefore be an ideal sensitizer for PDT if localization, pharmacokinetics and formulation variables were appropriate. Additional factors, pertinent to clinical applications, relate to the nature of the treatment field and of the site(s) of malignant disease.

A death mode termed paraptosis [17,18] has recently been implicated as a PDT response [19]. While paraptosis is usually associated with defective proteins in the ER, one report describes a paraptotic response after what appears to involve nuclear targeting [20]. Determinants and consequences of paraptosis are not fully understood. It has been proposed that chemotherapy leading to paraptosis may be a useful approach to cancer control [21,22]. Using PDT to explore paraptosis provides another example of the potential use of selective photodamage to explore death pathways.

There is as yet no biochemical assay for paraptosis. The associated morphology can be recognized by the appearance of multiple cytoplasmic vacuoles [17–22]. These are not autophagosomes, i.e., they have single membranes and their formation may be antagonized by brief exposure to agents that impair protein synthesis, e.g., actinomycin D or cycloheximide [17]. This report summarizes information on determinants of paraptosis and provides a further characterization of the process.

## MATERIALS AND METHODS

### Chemicals and supplies

BPD (benzoporphyrin derivative, Verteporfin) was provided by VWR (Cat No 1711461), Radnor PA. The chlorin NPe6, was obtained from Dr. Kevin M. Smith, Louisiana State University. Hypericin was purchased from BeanTown Chemical, Hudson NH. Photofrin was obtained from Pinnacle Biologics, Chicago IL. The pyropheophorbide HPPH was provided by Dr. R. Pandey, Roswell Park Cancer Institute; mTHPC was a gift from Prof. Ray Bonnett, Queen Mary College, London. Photofrin was generously provided by Pinnacle Biologics Inc. Other reagents were obtained from Sigma-Aldrich or Calbiochem Corp. and were of the highest available purity. Fluorescent probes used in this study were purchased from Thermo Fisher Scientific and Enzo Life Sciences, Farmingdale NY.

### Cell culture and clonogenic assays

OVCAR-5 cells were maintained in RPMI 1640 medium containing 10% fetal bovine serum. Methodology for carrying out clonogenic assays has been described [15]. Light doses required for photokilling in monolayer culture have been reported in prior studies from this laboratory [11,19]. To maintain an appropriate pH in the absence of CO2, irradiations were carried out in media buffered to pH 7.2 with HEPES. Viability was assessed by counting colonies of ~30 cells with an Oxford Optronix GelCount device. Although the GelCount software can readily detect colonies, crystal violet was used as an additional colony marker. All experiments were performed in triplicate.

### PDT protocols

Cells were grown on 22 × 22 mm cover slips in 35 mm sterile plastic dishes to near-confluent conditions. Cultures were incubated at 37°C with 20 μM NPe6, 0.5 μM BPD (each for one h) or with 1 μM hypericin, 1 μM HPPH, 0.5 μM mTHPC or 0.5 mg/ml Photofrin for 16 h. The medium was replaced and the dishes irradiated with a 600-watt quartz-halogen source (Cat. No. 66296-600Q-R07, Newport Corp., Irvine CA). The light beam was passed through a 10 cm layer of water to remove IR and the bandwidth confined by interference

filters (Newport, Irvine CA) to 650 ±10 nm (mTHPC), 660 ± 10 nm (NPe6, HPPH), 690 ± 10 nm (BPD), 630 ± 10 nm (Photofrin) or 600 ± 10 nm (hypericin) to initiate photodamage. Light doses were calculated using a Scientech H410 Power & Energy meter. Over a range from 600-700 nm at a 10 nm bandwidth, this light source provides irradiation at approx. 2 mW/sq cm. Light doses were 30 mJ/sq cm at 660 nm and 60 mJ/sq cm at 690 or 600 nm unless otherwise specified. To test for the effect of impaired protein synthesis, cycloheximide (5 μM) or salubrinal (50 μM) was added for a 4 h interval after irradiation. The morphologic response to other photosensitizing agents was assessed 4 h after irradiation using PDT doses that reduce viability by ~75%.

## Microscopy

Images were acquired with a Nikon E-600 microscope using a Rolera EM-CCD camera and MetaMorph software (Molecular Devices, Sunnyvale CA). At least 3 images were acquired for each sample, with typical representations shown here. A thermo-electrically cooled stage (15ºC) is used to minimize metabolic effects on photosensitizer localization or other phenomena. With an intensified CCD camera, exposures of 10-100 msec are feasible, minimizing photodynamic effects that might otherwise alter cellular morphology.

## Sub-cellular localization of hypericin

OVCAR-5 cells were incubated with 1 μM hypericin for 16 h at 37°C. ErTracker Green (ErTr), Lysotracker green (LTG) or Mitotracker green (MTG) were present (as specified) during the final 10 min at 500 nM concentrations. Fluorescence images were then obtained using 360-420 nm excitation and a 550 nm high-pass filter in the light path (hypericin) or with 440-500 nm excitation and a 650 lowpass filter in the light path (LTG, MTG, ErTr). Images were acquired with a Nikon E-600 microscope using a Rolera EM-CCD camera and MetaMorph software (Molecular Devices, Sunnyvale CA).

## Fluorescence assay for autophagy

The Enzo CYTO-ID autophagy detection kit was used following the instructions provided by the supplier. A proprietary fluorescent probe has been reported to label autophagosomes [23]. Cells were treated with 500 nM rapamycin + 5 μM chloroquine for 24 h to induce autophagosome formation as a control for autophagy detection. Probe fluorescence (520-550 nm) was detected upon excitation at 450-490 nm.

## Electron microscopy

Cells were trypsinized, the cell pellets fixed with glutaraldehyde and osmium tetroxide, treated with uranyl acetate + lead citrate, then dehydrated in ethanol. The resulting pellets were embedded in epon resin and cut with an ultramicrotome to a 70 nm thickness before viewing.

# RESULTS

## Hypericin localization

A comparison of fluorescence images obtained with OVCAR-5 cells using hypericin (red pixels) vs. ErTracker green shows an almost perfect correspondence. In contrast, there was minimal co-localization with MitoTracker green or LysoTracker green (Fig. 1). Localization of BPD (mitochondria and ER), NPe6 (predominantly lysosomes), mTHPC (ER) and HPPH (mitochondria and ER) have previously been reported [24,25].

## Chronology of paraptosis

Vacuole formation surrounding the nucleus can be detected as early as 4 h after an $LD_{90}$ PDT dose using hypericin as the photosensitizing agent. During the next 48 h, vacuoles become larger and eventually fill the cytoplasm. There was a substantial population of detached cells 48 h after irradiation; these showed a substantial loss of cytoplasm (Fig. 2).

## Effect of salubrinal

Exposure to 50 μM salubrinal for 4 hr after irradiation of cells photosensitized by hypericin led to a suppression of vacuole formation (Fig. 3). This did not, however, protect cells from a loss of viability (Fig. 4). Images acquired 20 h later revealed that vacuole formation had been delayed but not prevented (Fig. 3).

## Determinants of paraptosis

Effects of photodamage directed at various sub-cellular loci were further examined using three additional photosensitizing agents with known patterns of sub-cellular targeting [24,25]. These included the pyropheophorbide HPPH and mTHPC (both predominantly localized in the ER) and Photofrin (broad distribution that includes ER, lysosomes and mitochondria). Images acquired 4 h after $LD_{75\text{-}90}$ PDT doses show that lysosomal photodamage failed to elicit the cytoplasmic vacuolization associated with paraptosis, while photosensitizers that targeted ER for photodamage could elicit an early paraptotic response (Fig. 5).

## Autophagy vs. paraptosis

Autophagy also results in formation of cytoplasmic vacuoles. These have double membrane while vacuoles associated with paraptosis are bounded by single membranes. Images acquired 4 h after BPD-induced photodamage show the presence of vacuoles associated with both autophagy and paraptosis (Fig. 6). While there are several procedures for characterizing autophagy, we utilized a fluorescent probe provided by ENZO: Cyto-ID® Green autophagy dye (Fig. 7). There is evidence that this probe can label autophagosomes [23]. Data shown in Fig. 7 indicates that autophagosomes resulting from exposure of OVCAR-5 cells to rapamycin + chloroquine were labeled with this dye while those attributed to paraptosis were not. Rapamycin is a potent inducer of autophagy [26].

## DISCUSSION

Sub-cellular target(s) for photodamage vary among the different photosensitizing agents. The ability to select targets has proved useful both for optimizing photodamage and for investigation of pathways to cell death [7,11,15,19,25]. Photodamage leading to the loss of mitochondrial permeability barriers, permitting cytochrome c to migrate from photodamaged mitochondria to the cytoplasm and trigger apoptosis [27]. Agents with this targeting profile may also target the anti-apoptotic protein Bcl-2 for photodamage [28,29]. Lysosomal photodamage can allow proteases to migrate into the cytoplasm and cleave the protein Bid into a pro-apoptotic fragment that can promote apoptotic death [30].

We have proposed that a protocol that targets mitochondria + lysosomes can potentiate PDT efficacy [11,15,19]. While Photofrin has this spectrum of targeting activity [15], the long-wavelength absorbance band (630 nm) is sub-optimal for tissue penetration [16]. Lysosomal photodamage leads to release of $Ca^{2+}$ into the cytoplasm and activation of the enzyme calpain. This is followed by a calpain-catalyzed cleavage of the autophagy-associated protein ATG5 to form a pro-apoptotic fragment termed tATG5 that enhances the lethality of mitochondrial photodamage [11]. The initial report describing this pathway indicated that tATG5 can also promote the apoptotic response to chemotherapy [31]. In protocols we have utilized [11,15,19], prior or simultaneous lysosomal photodamage was found to enhance the efficacy BPD, a photosensitizing agent that targets both mitochondria and the ER [19]. Since the ER is also a reservoir of intracellular $Ca^{2+}$ [32], it might be expected that photodamage from BPD alone would be sufficient to trigger tATG5 formation. Perhaps only calcium stores in lysosomes are sufficiently mobile to migrate into the cytoplasm after photodamage.

There is, however, evidence that ER photodamage can initiate another death pathway termed paraptosis. In the first report describing this phenomenon, paraptosis was initiated by transfection with the human insulin-like growth factor I receptor (IGFR) and impaired by treatment with cycloheximide [17]. The latter agent interferes with protein synthesis [33]. Paraptosis can also be initiated by cyclosporin A and impaired by either cycloheximide or salubrinal [34]. The latter has been reported to protect cells from the effects of ER stress via inhibition of phosphatases that act on a translation initiation factor [35]. This leads to maintenance of protein phosphorylation and some protection from adverse effects of the unfolded protein response. There is evidence that paraptosis is triggered by misfolded ER proteins and is associated with enhanced expression of MAP kinases [17,18,34,36].

Since BPD targets both ER and mitochondria [19], we also examined hypericin for the study reported here. Hypericin is a more selective photosensitizing agent in the OVCAR-5 cell line, being quite specific for the ER (Fig. 1). Data shown here are consistent with ER localization in OVCAR-5 cells. While quenching effects could result in failure to detect fluorescence at certain sub-cellular loci, we have successfully detected localization of photosensitizers in lysosomes, mitochondria and ER [11,19]. If there are such ‘restricted’ loci, they do not include these structures. The requirement for continued protein synthesis for a rapid appearance of paraptosis is also true in the context of PDT: cycloheximide impaired vacuolization after photodamage catalyzed by BPD but could not restore viability [37]. Since improperly folded proteins in the ER are not cleared by cycloheximide,

preventing protein synthesis will not necessarily restore viability [36]. In an earlier study, we reported this to be true in the context of PDT [37]. We show here that salubrinal can only delay vacuole formation after ER photodamage (Fig. 3) and, like cycloheximide, fails to restore viability to photodamaged cells (Fig. 4).

Details on the nature of cell death associated with paraptosis are beginning to emerge [18,34,36]. The gradual degradation and loss of a significant portion of the cytoplasm leads to a residue of shrunken and non-viable cells that detach and float away. Paraptosis appears to play a role in the response to photodamage initiated by many photosensitizers in use today that include the ER among their sub-cellular targets (Fig. 5). We have detected the appearance of paraptosis to date only in monolayer culture. Further studies in 3D culture and *in vivo* will be needed to assess the role of paraptosis in PDT-induced cell death.

## Acknowledgments

Ann Marie Santiago provided valuable technical assistance during the duration of this study. Work described here was partly supported by NIH grant CA 23378 and by funds from the Office of the Vice President for Research at Wayne State University.

## References

1. Lipson RL, Baldes EJ, Gray MJ. 1967; Hematoporphyrin derivative for detection and management of cancer. Cancer. 20:2255–2257. [PubMed: 6073903]
2. Ho YK, Pandey RK, Missert JR, Dougherty TJ. 1990; Some components of the tumor-localizing fraction of hematoporphyrin derivative (1990). Photochem Photobiol. 52:1085–1088. [PubMed: 2150886]
3. Dougherty TJ, Gomer CJ, Weishaupt KR. 1976; Energetics and efficiency of photoinactivation of murine tumor cells containing hematoporphyrin. Cancer Res. 36:2330–2333. [PubMed: 1277138]
4. Hadjur C, Wagnières G, Ihringer F, Monnier P, van den Bergh H. 1997; Production of the free radicals O2- and .OH by irradiation of the photosensitizer zinc(II) phthalocyanine. J Photochem Photobiol B Biol. 38:196–202.
5. Agarwal ML, Clay ME, Harvey EJ, Evans HH, Antunez AR, Oleinick NL. 1991; Photodynamic therapy induces rapid cell death by apoptosis in L5178Y mouse lymphoma cells. Cancer Res. 51:5993–5996. [PubMed: 1933862]
6. Luo Y, Chang CK, Kessel D. 1996; Rapid initiation of apoptosis by photodynamic therapy. Photochem Photobiol. 63:528–534. [PubMed: 8934765]
7. Kessel D, Vicente MG, Reiners JJ. 2006; Initiation of apoptosis and autophagy by photodynamic therapy. Lasers Surg Med. 38:482–488. [PubMed: 16615135]
8. Reiners JJ, Agostinis P, Berg K, Oleinick NL, Kessel D. 2010; Assessing autophagy in the context of photodynamic therapy 2010. Autophagy. 6:7–18. [PubMed: 19855190]
9. Cincotta L, Szeto D, Lampros E, Hasan T, Cincotta AH. 1996; Benzophenothiazine and benzoporphyrin derivative combination phototherapy effectively eradicates large murine sarcomas. Photochem Photobiol. 63:229–237. [PubMed: 8657737]
10. Villanueva A, Stockert JC, Cañete M, Acedo P. 2010; A new protocol in photodynamic therapy: enhanced tumour cell death by combining two different photosensitizers. Photochem Photobiol Sci. 9:295–297. [PubMed: 20221454]
11. Kessel D, Evans CL. 2016; Promotion of proapoptotic signals by lysosomal photodamage: mechanistic aspects and influence of autophagy. Photochem Photobiol. 92:620–623. [PubMed: 27096545]
12. Kosharsky B, Solban N, Chang SK, Rizvi I, Chang Y, Hasan T. 2006; A mechanism-based combination therapy reduces local tumor growth and metastasis in an orthotopic model of prostate cancer. Cancer Res. 66:10953–10958. [PubMed: 17108133]

13. Allman R, Cowburn P, Mason M. 2000; Effect of photodynamic therapy in combination with ionizing radiation on human squamous cell carcinoma cell lines of the head and neck. Br J Cancer. 83:655–661. [PubMed: 10944608]
14. Razum N, Balchum OJ, Profio AE, Carstens F. 1987; Skin photosensitivity: duration and intensity following intravenous hematoporphyrin derivatives, HpD and DHE. Photochem Photobiol. 46:925–928. [PubMed: 2964669]
15. Kessel D. 2016; Photodynamic therapy: promotion of efficacy by a sequential protocol. J Porph Phthalo. 20:302–306.
16. Wilson BC, Jeeves WP, Lowe DM. 1985; In vivo and post mortem measurements of the attenuation spectra of light in mammalian tissues. Photochem Photobiol. 42:153–162. [PubMed: 4048297]
17. Sperandio S, de Belle I, Bredesen DE. 2000; An alternative, nonapoptotic form of programmed cell death. Proc Natl Acad Sci. 97:14376–14381. [PubMed: 11121041]
18. Sperandio S, Poksay KS, Schilling B, Crippen D, Gibson BW, Bredesen DE. 2010; Identification of new modulators and protein alterations in non-apoptotic programmed cell death. J Cell Biochem. 111:1401–1412. [PubMed: 20830744]
19. Kessel D, Reiners JJ. 2017; Effects of combined lysosomal and mitochondrial photodamage in a non-small-cell lung cancer cell line: the role of paraptosis. Photochem Photobiol. 93:1502–1508. [PubMed: 28696570]
20. Pierroz V, Rubbiani R, Gentili C, Patra M, Mari C, Gasser G, Ferrari D. 2016; Dual mode of cell death upon the photo-irradiation of a RuII polypyridyl complex in interphase or mitosis. Chem Sci. 7:6115–6124. [PubMed: 27708751]
21. Guamán-Ortiz LM, Orellana MI, Ratovitski EA. 2017; Natural compounds as modulators of non-apoptotic cell death in cancer cells. Curr Genomics. 18:132–155. [PubMed: 28367073]
22. Park SS, Lee DM, Lim JH, Lee D, Park SJ, Kim HM, Sohn S, Yoon G, Eom YW, Jeong SY, Choi EK, Choi KS. 2018; Pyrrolidine dithiocarbamate reverses Bcl-xL-mediated apoptotic resistance to doxorubicin by inducing paraptosis. Carcinogenesis. 39:458–470. [PubMed: 29329420]
23. Chan LL, Shen D, Wilkinson AR, Patton W, Lai N, Chan E, Kuksin D, Lin B, Qiu J. 2012; A novel image-based cytometry method for autophagy detection in living cells. Autophagy. 8:1371–1382. [PubMed: 22895056]
24. Marchal S, François A, Dumas D, Guillemin F, Bezdetnaya L. 2007; Relationship between subcellular localisation of Foscan and caspase activation in photosensitised MCF-7 cells. Br J Cancer. 96:944–951. [PubMed: 17325708]
25. Kessel D. 2004; Correlation between subcellular localization and photodynamic efficacy. J Porph Phthalo. 8:1009–1014.
26. Renna M, Jimenez-Sanchez M, Sarkar S, Rubinsztein DC. 2010; Chemical inducers of autophagy that enhance the clearance of mutant proteins in neurodegenerative diseases. J Biol Chem. 285:11061–11067. [PubMed: 20147746]
27. Kessel D, Lou Y. 1999; Photodynamic therapy: a mitochondrial inducer of apoptosis. Cell Death Differ. 6:28–35. [PubMed: 10200545]
28. Kim HR, Luo Y, Li G, Kessel D. 1999; Enhanced apoptotic response to photodynamic therapy after bcl-2 transfection. Cancer Res. 59:3429–3432. [PubMed: 10416606]
29. Xue LY, Chiu SM, Oleinick NL. 2001; Photochemical destruction of the Bcl-2 oncoprotein during photodynamic therapy with the phthalocyanine photosensitizer Pc 4. Oncogene. 20:3420–3427. [PubMed: 11423992]
30. Reiners JJ, Caruso JA, Mathieu P, Chelladurai B, Yin XM, Kessel D. 2002; Release of cytochrome c and activation of pro-caspase-9 following lysosomal photodamage involves Bid cleavage. Cell Death Differ. 9:934–944. [PubMed: 12181744]
31. Yousefi S, Perozzo R, Schmid I, Ziemiecki A, Schaffner T, Scapozza L, Brunner T, Simon HU. 2006; Calpain-mediated cleavage of Atg5 switches autophagy to apoptosis. Nat Cell Biol. 8:1124–1132. [PubMed: 16998475]
32. Koch GL. 1990; The endoplasmic reticulum and calcium storage. Bioessays. 12:527–531. [PubMed: 2085319]
33. Siegel MR, Sisler HD. 1963; Inhibition of protein synthesis in vitro by cycloheximide. Nature. 200:675–676. [PubMed: 14109947]

34. Ram BM, Ramatishna G. 2014; Endoplasmic reticulum vacuolation and unfolded protein response leading to paraptosis like cell death in cyclosporine A treated cancer cervix cells is mediated by cyclophilin B inhibition. Biochim Biophys Acta. 1843:2497–2512. [PubMed: 25003316]

35. Boyce M, Bryant KF, Jousse C, Long K, Harding HP, Scheuner D, Kaufman RJ, Ma D, Coen DM, Ron D, Yuan J. 2005; A selective inhibitor of eIF2alpha dephosphorylation protects cells from ER stress. Science. 307:935–939. [PubMed: 15705855]

36. Wang L, Gundelach JH, Bram RJ. 2017; Cycloheximide promotes paraptosis induced by inhibition of cyclophilins in glioblastoma multiforme. Cell Death Dis. 8:e2807. [PubMed: 28518150]

37. Kessel, D, Cho, W-J, Kim, HR-C. Photodynamic Therapy: the Role of Paraptosis. Proc SPIE In Press; 2018.

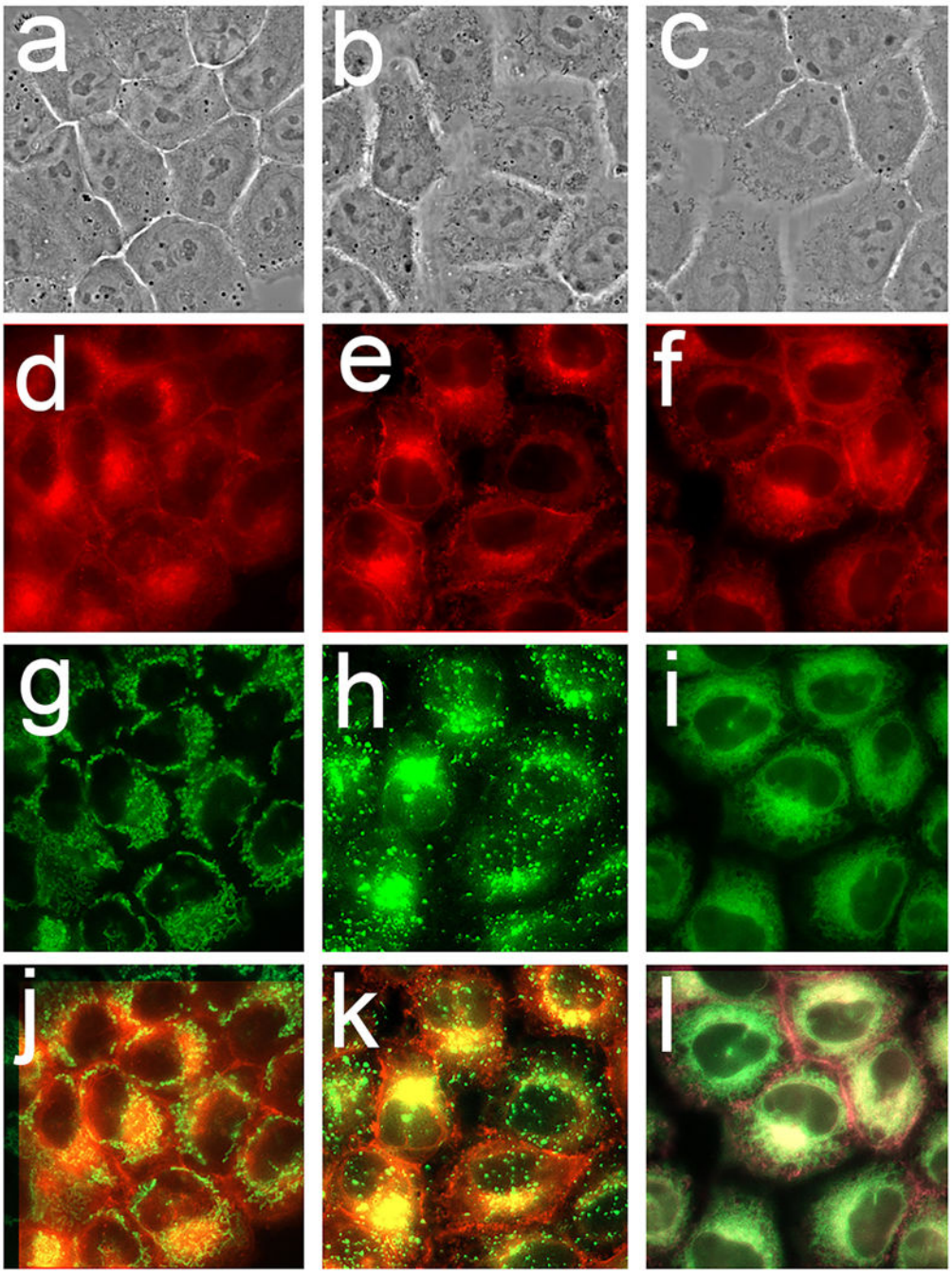


**Figure 1.**

Localization of hypericin in OVCAR-5 cells. Phase-contrast images (a-c) hypericin labeling (d-f), fluorescent probes (g-i) and overlays of hyupericin + probes (j-l) are shown. The fluorescent probes are MitoTracker green (g), LysoTracker green (h) and ErTracker green (i). Overpays of hypericin + probes are shown in the bottom panels: hypericin + MTG (j), hypericin + LTG (k) and hypericin + ErTrG (l).

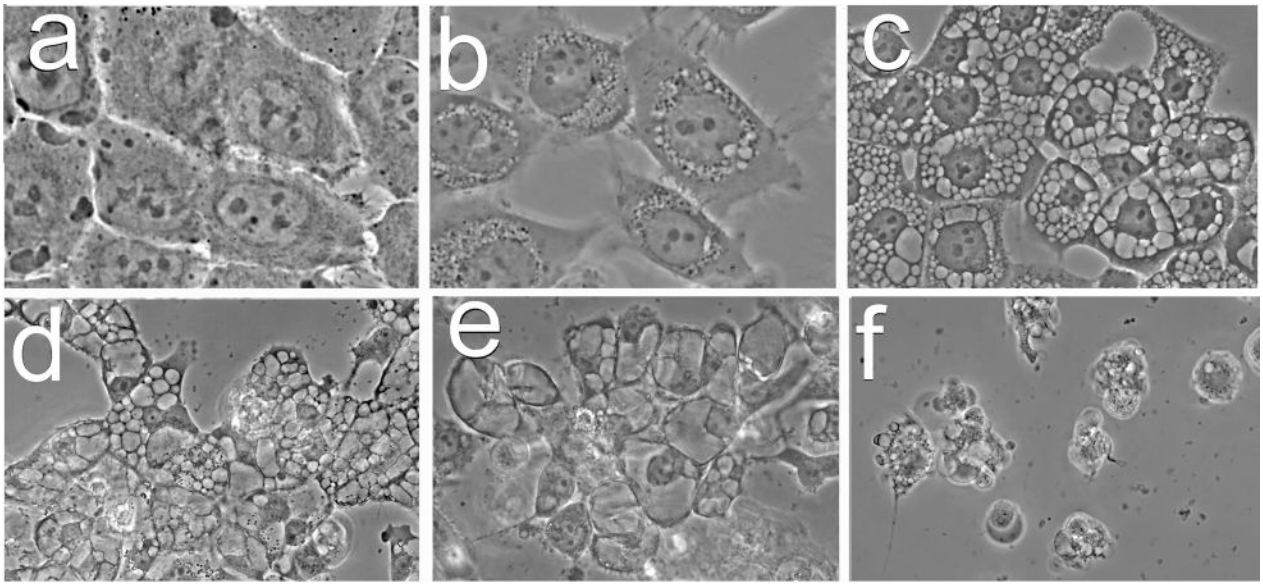


**Figure 2.**

The chronology of paraptosis. Images were acquired sequentially after irradiation of OVCAR-5 cells photosensitized with hypericin as described in the text. Legend: a, before irradiation; b-f, images acquired after irradiation (180 mJ/sq cm at 600 nm): b, 1 h; c, 4 h; d, 24 h; e, adhering cells after 48 h; f, floating cells after 48 hr.

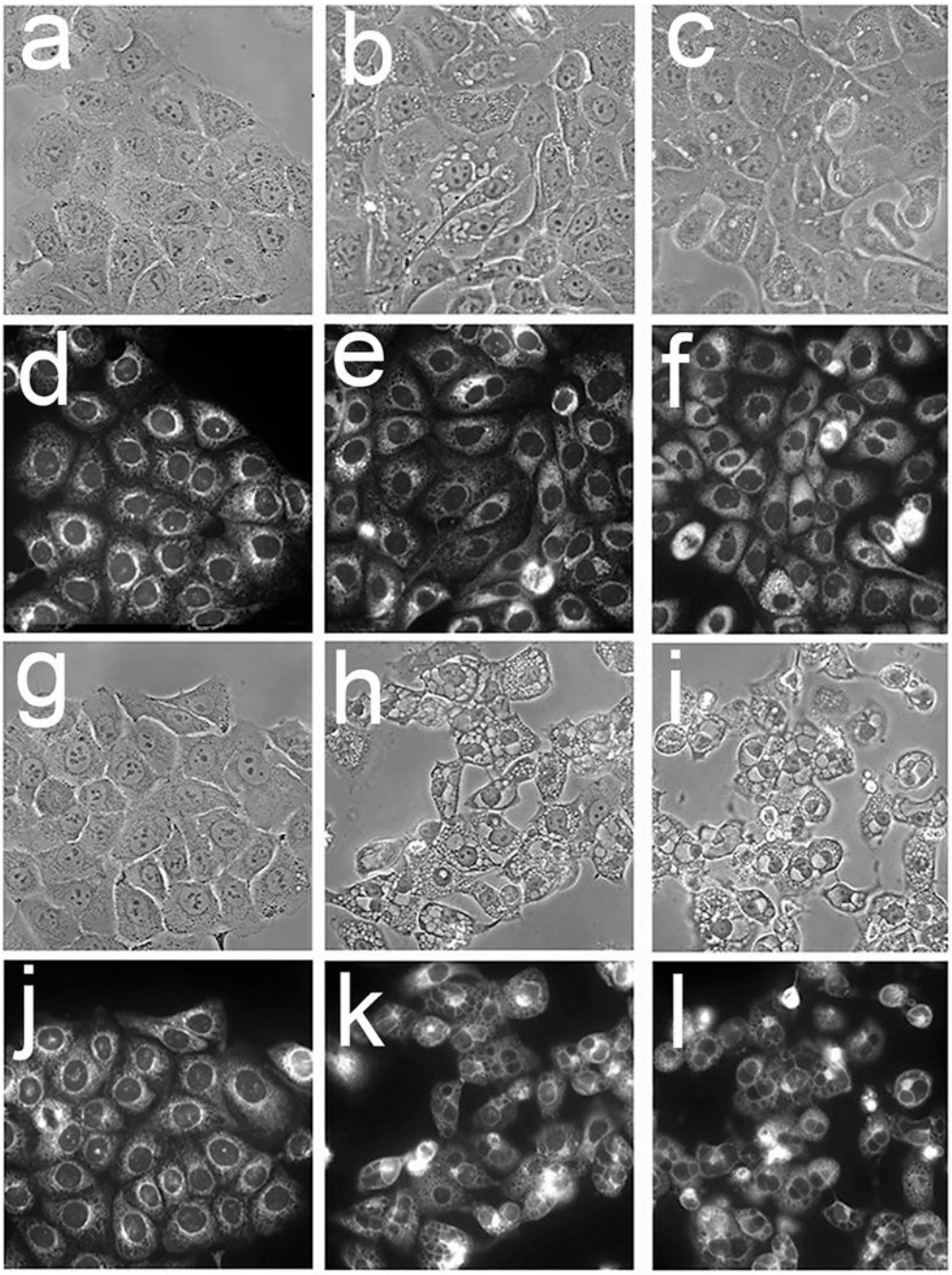


**Figure 3.**

OVCAR-5 morphology and patterns of ErTracker green labeling of untreated cells and cells 4 h and 24 h after irradiation. Cells were photosensitized with hypericin and irradiated (180 mJ/sq cm at 600 nm). The left series of panels (a, d, g, j) depicts controls, central panels (b, e, h, k) show the effect of photodamage, right panels (c, f, I, l) indicate results obtained when salubrinal (50 μM) was present for 4 hr after irradiation. Images in panels a-f were acquired 4 hr after irradiation; in panels g-l 24 hr after irradiation.

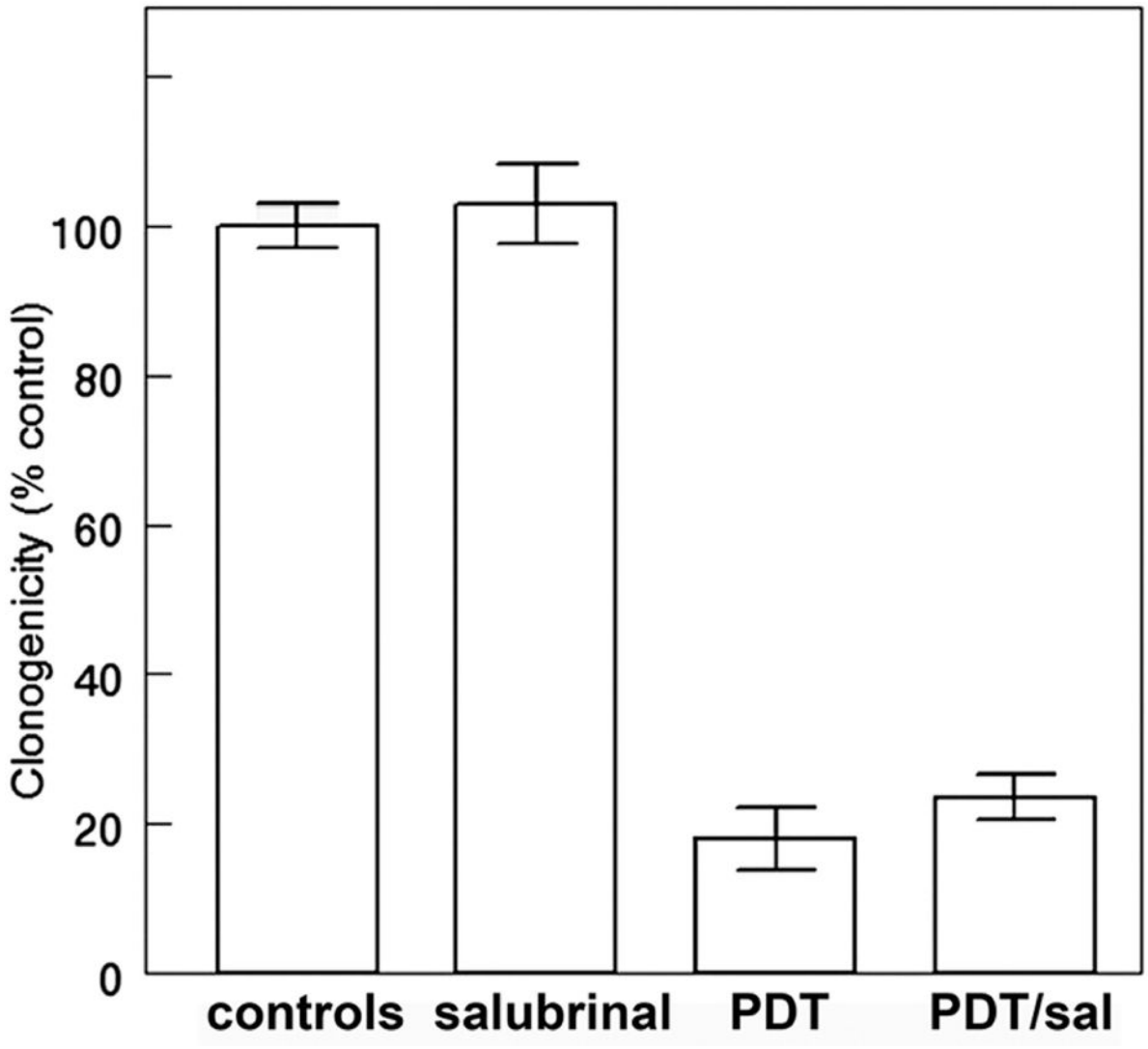


**Figure 4.**

Effect of salubrinal on OVCAR-5 clonogenicity using conditions described in the legend to Fig. 3. Each bar represents values obtained in 3 replicate experiments. Cells were photosensitized with hypericin and irradiated (180 mJ/sq cm at 600 nm).

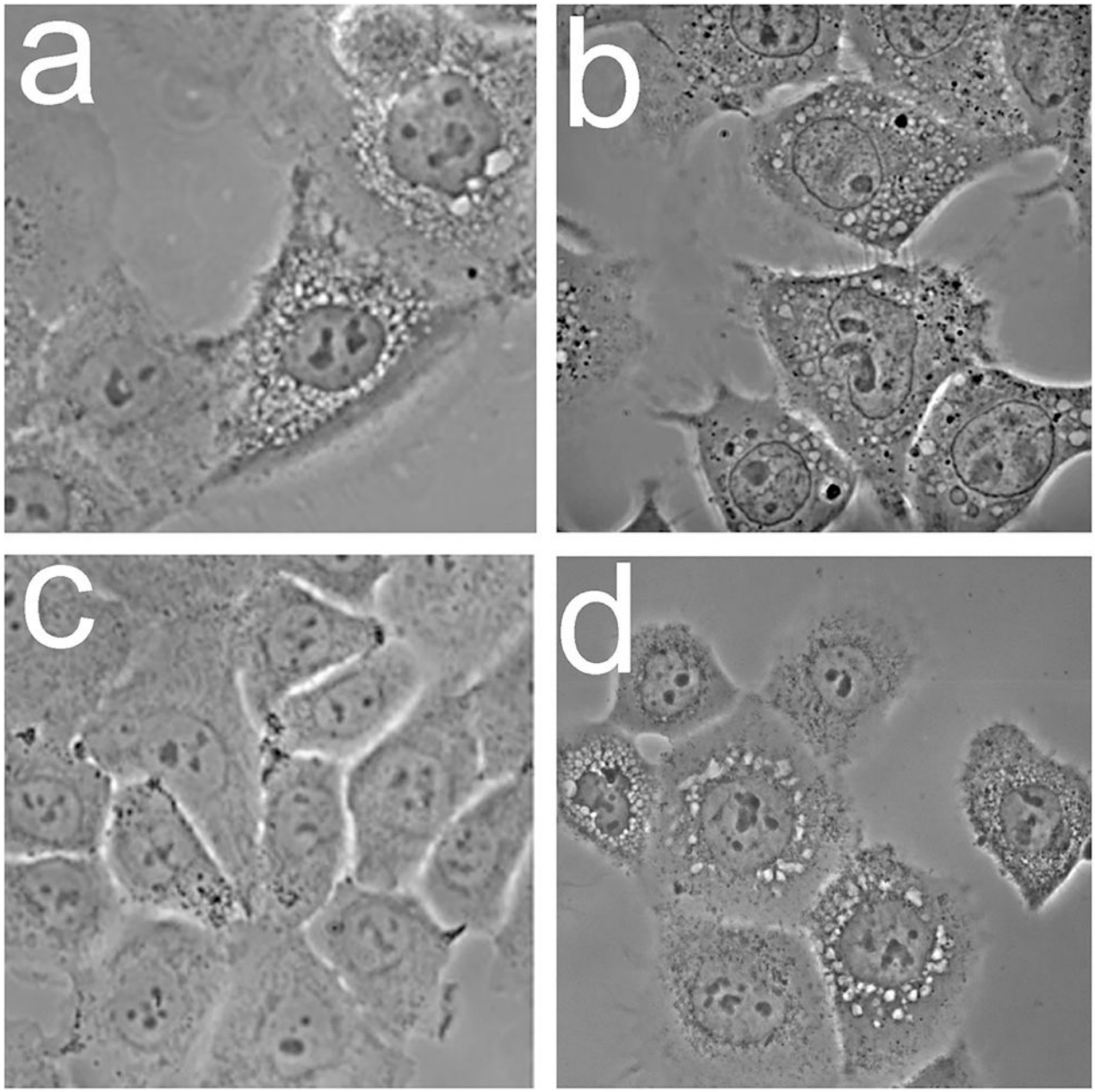


**Figure 5.**

Morphology of OVCAR-5 cells 4 h after photodamage from: a, mTHPC, b, Photofrin; c, NPe6; d, HPPH. In each case, the corresponding loss of viability was 75-90%.

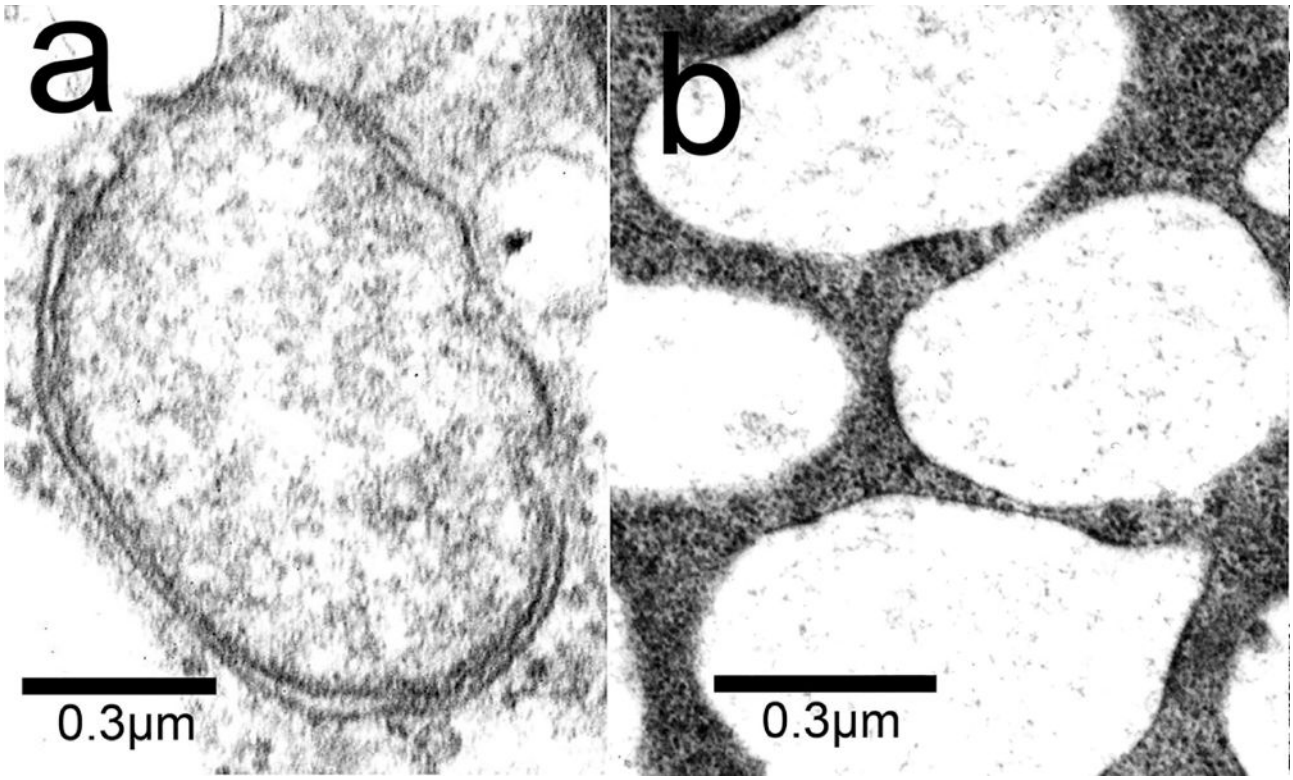


**Figure 6.**
Electron microscopy showing the morphology of autophagy vs. paraptosis in cells 4 h after being photosensitized with BPD ($LD_{50}$ conditions) and irradiated.

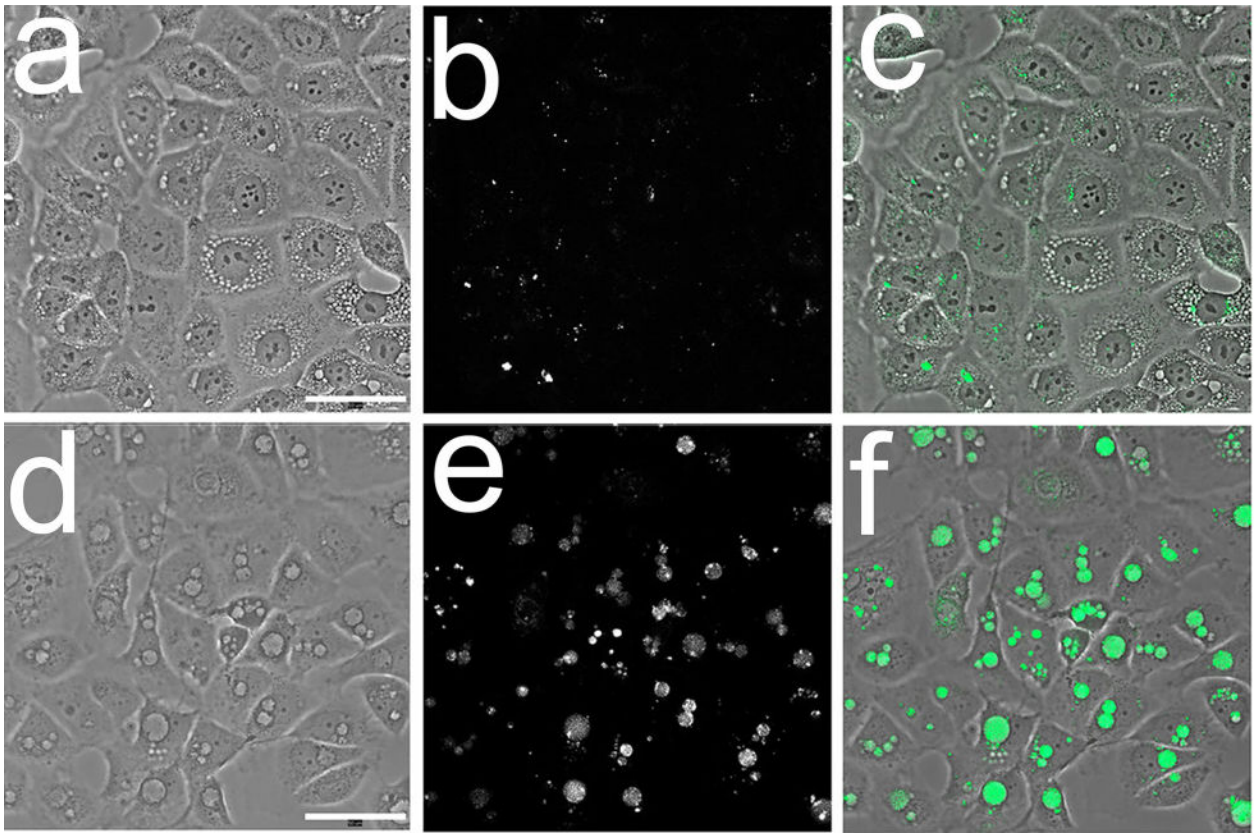


**Figure 7.**

Probing OVCAR-5 cells for autophagy with Cyto-ID® Green. Images were acquired 4 h after the specified treatment. Top row: hypericin-induced photodamage: a, phase-contrast, b, probe fluorescence; c, overlay. Bottom row: images acquired after treatment with 500 nM μM Rapamycin + 5 μM chloroquine: d, phase-contrast; e, probe fluorescence; f, overlay.